Biophysical Aspects of Auger Processes, AAPM Symposium Series No. 8 (1992) 249-272
Eds. RW Howell, VR Narra, KSR Sastry, DV Rao

TISSUE, CELLULAR, AND SUBCELLULAR DISTRIBUTION OF INDIUM RADIONUCLIDES IN THE RAT

BO-ANDERS JÖNSSON, SVEN-ERIK STRAND, HADAR EMANUELSSON[1], and BENGT LARSSON[2]

Departments of Radiation Physics and Zoophysiology[1]
University of Lund, Sweden

Department of Toxicology[2]
University of Uppsala, Sweden

ABSTRACT

The tissue distribution of ^{111}In-activity in rat organs after intravenous injections of different ^{111}In-radiopharmaceuticals have been studied by autoradiography. Quantitation was performed utilizing an image analyzing system designed for local measurements on whole-body autoradiographs. Additional studies of the cellular and subcellular localization in testes and bone marrow were performed by light and electron microscopy autoradiography after injection of ^{114m}In. The whole-body autoradiographs demonstrated a marked inhomogeneous radionuclide distribution in various tissues (*e.g.* kidneys, spleen, liver, bone marrow, lymph nodes and testes). In the testes it was observed by light microscopy autoradiography that the activity was localized in a significant concentration in the interstitial tissue, and to a minor amount in the periphery of the seminiferous tubules, coincident with the location of the radiosensitive spermatogenic cell lineage. In electron microscope autoradiographs subcellular localization sites appeared near and within the cell nucleus of spermatogonial cells, and also close to mitochondria. Similar results were found in the bone marrow. Our experiments show that the distribution pattern may have a significant impact

Published by American Institute of Physics, Inc., Woodbury, NY 11797

on calculation of the local absorbed dose to organs or individual cells when conventional dosimetry is employed. In the light of the increased interest in energy deposition at the cellular level, the present investigation suggests that autoradiographic techniques are excellent for acquiring localization data necessary for cell-level dosimetry calculations.

INTRODUCTION

The average absorbed dose to a tissue or organ in the body comprises the basic data necessary for risk estimates. The procedures outlined by MIRD, ICRU and ICRP (1-3) assume that the radionuclide, as well as the total energy imparted[a] (4), are uniformly distributed in organs or tissues. Thus, the absorbed dose to all cells in the organ is the same as the calculated mean absorbed dose to the organ. Heterogeneously distributed activity within an organ is not considered. In the case of radionuclides emitting low energy electrons (*i.e.* conversion-, Auger-, and Coster-Kronig electrons), special attention should be paid to the cellular distribution and subcellular decay sites (5-8). In addition to the two γ-rays with energies of 171 and 245 keV, and X ray photons of approximately 24 keV, ^{111}In emits numerous low energy electrons as given in Table I (9), which deposit their energy in small volumes ranging from a few nm for Auger electrons (10) to several cell diameters for the conversion electrons (11).

Many radiopharmaceuticals have, during the two last decades, been labeled with ^{111}In. In the early 1970's, efforts using ^{111}In-chloride for diagnosis of tumors (12-15) and for erythroid marrow scintigraphy (16,17) were performed. Later, different ^{111}In-chelates (*i.e.* oxine[b], tropolone[c], and MERC[d]) were introduced for labeling of different blood cells *in vitro* (18-27). During the 1980's tumor-imaging using labeled monoclonal antibodies expanded considerably, and ^{111}In is still the radionuclide of choice (28-34). Recently blood cell specific monoclonal antibodies labeled with ^{111}In for non-tumor imaging have also been developed (35-40).

---

[a]For radiation protection purposes, the tissue- or organ-average absorbed dose, D_T, is defined as $D_T = \varepsilon_T / m_T$ where ε_T is the total energy imparted in tissue or organ and m_T is the mass of that tissue or organ. The SI unit for absorbed dose is J/kg or Gy.

[b]In-111-TRIS-8-hydroxyquinoline

[c]In-111-2-hydroxy-2,4,6-cycloheptatrenine

[d]In-111-2-Mercaptopyridine-N-Oxide

TABLE I

^{111}In Average Radiation Spectrum[e]

Radiations	Average Energy (keV)	Yield per decay	Range[f] (μm)
Photons			
γ_1	171.3	0.902	
γ_2	245.3	0.940	
K_α X rays	23.1	0.680	
K_β X rays	26.2	0.146	
Conversion electrons			
K-shell, γ_1	114.6	0.0841	194
L,M,N-shells, γ_1	168.0	0.0130	254
K-shell, γ_2	218.6	0.0503	386
L,M,N-shells, γ_2	242.1	0.0097	445
Auger electron groups			
KLL	19.17	0.1059	8
KLX	22.32	0.0455	10
KXY	25.44	0.0059	13
LXY	2.81	1.0178	0.33
MXY	0.51	1.91	0.03
NXY	0.12	1.13	0.005
Coster-Kronig electron groups[g]			
L-shell	0.182	0.149	0.008
M-shell	0.039	0.925	< 0.002
N-shell	0.012	2.54	<0.001

[e]In-111 decays by electron capture with a half-life of 2.83 d. For a complete decay scheme see Ref. 9.

[f]Ranges for conversion electrons are taken from Ref. 11 and is the x_{90} value (*i.e.* the radius of a sphere in which 90% of the electron energy is absorbed) Ranges for Auger- and Coster Kronig electrons are calculated from Ref. 10.

[g]Data taken from Ref. 48.

Although it is likely that many radiopharmaceuticals are not distributed homogeneously and concentrate in parts of an organ, and in or adjacent to specific cells, only few studies have dealt with tissue and cellular localization studies after intravenously injected radiopharmaceuticals (41-43). For radiosensitive cells in organs such as the reproductive systems or the red bone marrow, localization studies are of prime importance. Recent radiobiological *in vivo* experiments have demonstrated that ^{111}In may have severe radiotoxicity to cells. The deleterious effect of ^{111}In was first noticed after ^{111}In-oxine labeling of lymphocytes (44-46). The radionuclide was found to bind firmly to cellular components and to some extent to DNA (47). The first experiment showing the enhanced biological effect of ^{111}In *in vivo* was reported by Rao *et al.* (48,49) where the cytotoxicity of ^{111}In-oxine, ^{111}In-citrate, and ^{114m}In-citrate were studied using mouse spermatogenesis and oogenesis as the models. They reported a significant decrease in survival of sperm heads and loss in the testes weight after intratesticular injection of ^{111}In-oxine. Similar results have been found in rat testes after intratesticular injection of oxine labeled with either ^{111}In (50) or ^{110}In (51). Later it has also been reported that internalized ^{111}In induced sperm head abnormalities (52). Few published studies, however, have demonstrated activity in the testicular cells after intravenously administered ^{111}In-radiopharmaceuticals. After intravenous injections of ^{111}In labeled compounds, a small portion (~ 0.5%) of the injected activity localizes in the testes and clears with a prolonged effective half-life (53,54). Jackson *et al.* (55) found that after injection of ^{114m}In labeled leukemia cells, minute amounts of ^{114m}In deposited in the testes and entirely destroyed the seminiferous tubules by 120 days. They also reported that ^{114m}In-oxine in plasma damaged the stem cell spermatogonia.

Consequently, there may be good reasons to suspect an inhomogeneous distribution and long term accumulation of indium isotopes in the testes, and that the indium atoms can be internalized by various cells. To date, no studies have reported data relevant to nuclear medicine practice (*i.e.* on the cellular distribution in the testes or other organs after intravenous injection of ^{111}In labeled radiopharmaceuticals).

The structure of the mammalian testes is characterized by the seminiferous tubules and the interstitial tissue (56). The epithelium consists of supporting Sertoli cells and cells that constitute the spermatogenic lineage (*i.e.* spermatogonial stem cells, differentiating spermatogonia, spermatocytes, spermatids and spermatozoa). The spermatogonia represent the proliferative stage of spermatogenesis and are identified as very radiosensitive cells (57,58).

The Sertoli cells are found in the basal membrane of the seminiferous tubules extending towards the lumen. These cells maintain a microenvironment suitable for the spermatogenic cells. The space between the seminiferous tubules is occupied by interstitial cells (*i.e.* Leydig cells and tissue macrophages, as well as connective tissue, nerves, blood and lymphatic vessels).

The International Commission on Radiological Protection (ICRP) (59,60), approximates the uptake of ionic indium as being divided between four major organs; kidneys (0.07), liver (0.2), red bone marrow (0.3) and spleen (0.01). The remaining fraction is assumed to be uniformly distributed through all other organs and tissues in the body. The red bone marrow is of significant importance for radiation protection. The bone marrow is, after the blood itself, the largest and most widely dispersed tissue in the body. The two components recognized in the bone marrow are hematopoietic cords that comprise the majority of the cellular elements, and the stroma cells that support the proliferation of hematopoietic cells. Different cells, including erythrocytes, granular leukocytes, monocytes, and platelets, are derived from stem cells in the red bone marrow, which are known to be very radiosensitive (61,62). Since ^{111}In, now recognized as radiotoxic when accumulated in the testes, is also taken up in a considerable amount in the red bone marrow, more detailed studies of the tissue and cellular localization after intravenous injections of ^{111}In-labeled agents are extremely important.

Here we report results from investigations of the activity distribution in various organ after intravenous administration of ^{111}In-radiopharmaceuticals into rats. Whole-body autoradiography (WBARG) as well as studies of the cellular and subcellular localization using light- and electron microscope autoradiography (LMARG and EMARG) were performed on testes and red bone marrow. In the cellular case we used ^{114m}In because of its longer half-life.

MATERIALS AND METHODS

Macro-autoradiography

Male Wistar rats (MOELLEGAARD Breeding Centre, Denmark) weighing approximately 220 g were used in this study. The animals had free

access to food and water *ad libitum*. Animals were sacrificed by inhalation of carbon dioxide.

The animals were given intravenous injections (0.2 ml) of either 18.5 MBq ^{111}In-chloride (pH 2), ^{111}In-oxine, or ^{111}In-tropolone (Mallinckrodt Diagnostica, Petten, Holland), or 25 MBq of ^{111}In-CEA-F(ab')$_2$ BW431/31 (Scintimun®, Behringwerke, Marburg, Germany). The method used for whole-body autoradiography (WBARG) has been given in detail elsewhere (63) and is only described briefly. Five days after injection the rats were killed and immediately immersed in a -70°C freezing mixture of liquid hexane and solid carbon dioxide for 5 min. The animal was then horizontally attached to a cryomicrotome stage surrounded by a metal frame and embedded in carboxymethyl cellulose (CMC) by freezing in hexane. From the animals 25 sections each 20 and 60 µm thick were cut with a cryomicrotome (LKB PMV 2250) and picked-up on an adhesive tape (Scotch 3M No. 810). After freeze-drying the sections were attached to X-ray films (Structurix D7, Agfa-Geavert, Germany) and put into cassettes. After an exposure time of 2 weeks the films were developed and fixed.

The autoradiographs from the WBARG-rats were analyzed with a digital image analyzing system especially adapted for whole-body autoradiography (64). The image sampling device was a video-camera (Phillips LDH 400/61) on an adjustable mounting above a light box (Novalux A4E, Photron, Sweden). The video signal was transferred to a microcomputer (Cromemco System 2-HD) via an image digitizer (384 X 241 pixels and 256 gray levels). Using a digitizer pad, regions of interest (ROI) were indicated on a stored autoradiographic image, and the gray-level distribution displayed as a pixel histogram (y-axis) as a function of the gray-levels (x-axis).

All autoradiographs were examined qualitatively, searching for activity uptakes and distribution patterns in various tissues and organs. Selected autoradiographs were examined in detail quantitatively using the digital imaging system. After a software controlled calibration for accurate measurements of the optical density, several consecutive autoradiographs were digitized and images stored in the computer. The contrast of the image was enhanced and regions of interest (ROI) were chosen over a specific organ to generate a histogram representing the gray-scale distribution (*i.e.* the number of pixels as a function of optical density). The histogram was scanned with different selected "windows" and detailed information about the location, mean optical density and its standard deviation, and the number of

pixels within the selected window were displayed. The optical density of consecutive small selected windows was, after correction for background density, divided by the mean optical density for the whole ROI area. Thus, an estimate of the activity concentration ratios in different parts of the organ was obtained. The activity distribution was then expressed as the fraction of a tissue area with a specific activity concentration ratio (65).

Micro-autoradiography

One rat was intravenously injected with 18.5 MBq ^{114m}In-chloride in 0.5 M HCl (DuPont de Nemours & Co. Inc., Wilmington, Delaware, USA) in a volume of 0.2 ml. Twenty four hours after injection the rat was killed and small samples (1-2 mm^3) from the testes and from the bone marrow of the femur were rapidly removed and immediately fixed in 2.5% glutaraldehyde in 0.1 M sodium cacodylate buffer (pH 7.2, 1 h, 4°C). Post-fixation was done in 1% osmium tetroxide in the same buffer (1 h, 4°C). After rinsing, the tissue fragments were dehydrated in graded series of acetone, embedded in Epon overnight, and finally sectioned for light and electron microscope autoradiography.

For light microscope autoradiography 1 μm sections were covered with in ILFORD K2 liquid nuclear emulsion according to the dipping method, and the autoradiographs were exposed for 2-4 weeks at 4°C. They were developed in Kodak D-19 (5 min, 18°C), briefly rinsed in distilled water, and fixed in Kodak F-24 (6 min, 18°C). After a final rinsing, they were stained through the film with Richardson's azure II and methylene blue, and mounted in DePeX.

The ultrathin sections for electron microscope autoradiography were first coated with a monolayer of ILFORD L4 liquid nuclear emulsion according to the loop method and exposed for 1-3 months at 4°C. The autoradiographs were developed in Kodak D-19 (2 min, 20°C), rinsed in distilled water (30 s, 20°C), fixed in newly made 15% $Na_2S_2O_3$ (3 min, 20°C), and finally washed in distilled water. They were examined with a JEOL 100CX electron microscope at the Unit of Electron Microscopy, Department of Zoology, University of Lund. Control samples from an unlabeled animal were fixed and prepared for autoradiography in exactly the same manner as the radiolabeled samples. The background level of silver grains in these autoradiographs was insignificant.

A total of 20 autoradiographs of germ cells from different parts of the seminiferous tubule and from the red bone marrow were documented in a systematic random manner.

RESULTS

The patterns of activity distribution for ^{111}In after intravenous injections into rats are almost the same after a few days regardless of the radiopharmaceutical injected. In general, numerous tissues contain significant uptake of ^{111}In which can be seen in Fig. 1A. The whole-body autoradiograph in panel A shows the activity distribution after injection of ^{111}In-chloride, and is also representative for the other substances injected. ^{111}In is strongly accumulated in rapidly proliferating tissues such as bone marrow, intestinal walls, testes, skin, and the pulp cavity of the incisor teeth. High concentrations of activity are also found in the liver and spleen. No blackening at all is seen over the brain or in the intestines. The major difference between the different radiochemicals is the rate of blood elimination which is relatively slow after injection of ^{111}In-oxine (54). This is because ^{111}In-oxine very rapidly labels circulating erythrocytes, resulting in a longer retention time. For the other substances, however, the blood elimination is fast and no activity can be seen in the blood (see heart chamber in Fig. 1).

The autoradiographic results are confirmed by biokinetic studies (53,54) with the same substances used in the present study. Almost the same activity concentrations were found in various organs at day 5 regardless of the compound injected (Table II). A large difference was found, however, for the uptake in liver and spleen in the case of ^{111}In-oxine which was due to the labeled erythrocytes as mentioned above. In other autoradiographic experiments we also found a considerable accumulation in the liver and spleen after injection of ^{111}In-labeled leukocytes and platelets (data not presented).

A marked heterogeneous distribution of ^{111}In-activity is found in some organs. The distribution in the testes is complex (Fig. 1, panel B). In the bone marrow (Fig. 1, panel C) several hot spots were found, while in the spleen (Fig. 1, panel D) activity is mainly localized in the red pulp. Histograms from quantitatively examined autoradiographs of saggital sections of the testes, bone marrow, and spleen are presented in Figs. 2A-2I for the ^{111}In-

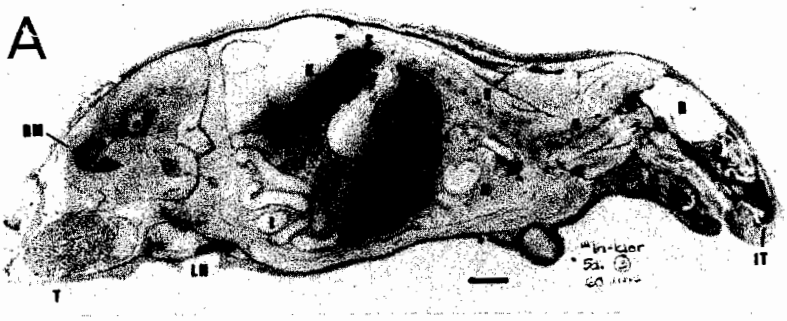

FIG. 1A. Representative whole-body autoradiograph of a rat 5 days after I.V. injection of ^{111}In-chloride. Significant concentrations of activity are seen in numerous organs. It should be noted that many of the organs that accumulated ^{111}In are characterized by areas of rapid cell proliferation. Abbreviations are; T=testes, BM=bone marrow, K=kidney, LN=lymph nodes, L=liver, V=vertebrae (bone marrow) S=spleen, I=intestines, H=heart, B=brain, and IT= incisor teeth (pulp cavity). Bar=10mm.

FIG. 1B. Illustration of the marked heterogeneous distribution of activity in the testes. The activity which has been transported into the testes as ^{111}In-transferrin is mainly localized in a network pattern, apparently representing the tubule of the testes. The image is contrast enhanced for clarity.

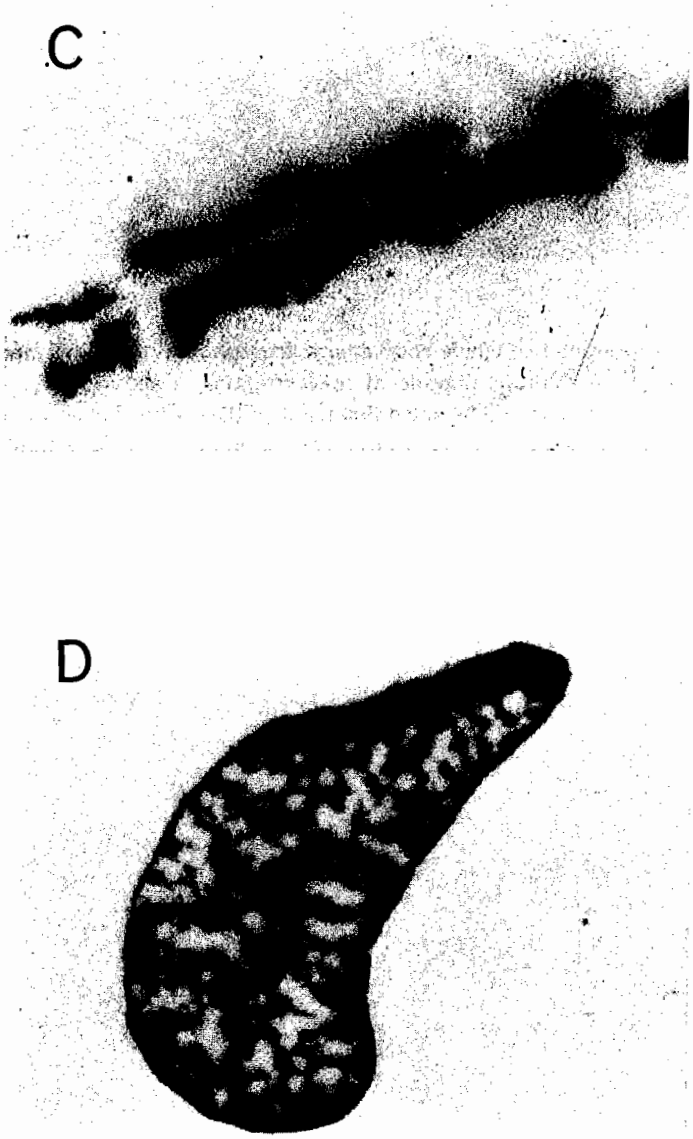

FIGS. 1C-1D. Illustrations above show the marked heterogeneous distribution of activity in the bone marrow in vertebral column (panel C), and spleen (panel D). The red and white pulp in the spleen are easily distinguished. Images are contrast enhanced for clarity.

radiopharmaceuticals. The diagrams illustrate the fraction of pixels in an ROI with a specific optical density, normalized to the mean optical density of the whole ROI-area (typically the whole tissue area of the autoradiograph). The width of the bars is approximately one standard deviation. In this manner, an estimation of the heterogeneity in the organ may be made at a macroscopic level. It should be noted that a similar pattern was found regardless of the radiocompound. In the testes (Figs. 2A-2C) at least half of the area has an optical density equal to that of the mean, although there were areas with significantly greater or lesser optical density. In the bone marrow (Figs. 2D-2F) about one third of the area corresponds to the mean optical density and several hot or cold spots are located irregularly in the tissue. The optical

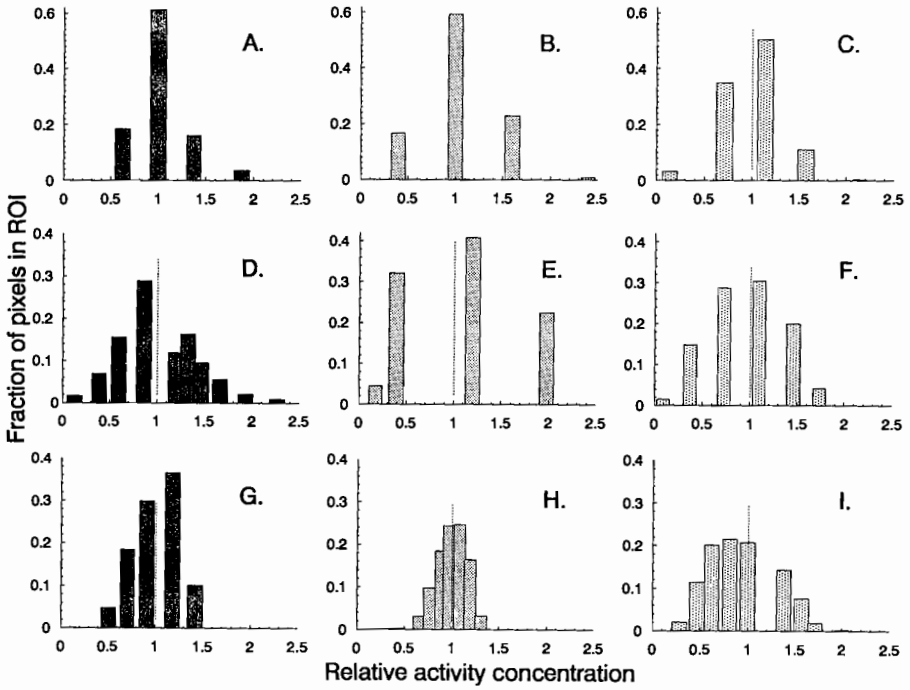

FIG. 2. Diagrams showing the fraction of pixels in an ROI with a measured optical density (specific activity) normalized to the mean optical density of the whole ROI. Left column: ^{111}In-chloride; middle column: ^{111}In-oxine; and right column: ^{111}In-CEA-F(ab')$_2$. Histograms A-C testes, D-F red bone marrow, and G-I spleen. The width of the bars is one standard deviation.

density of the spleen image (Figs. 2G-2H) is symmetrically scattered around the mean optical density, meaning that the organ contains either black or white areas that correspond to either abundant or deficit activity relative to the mean.

Representative autoradiographs of the activity uptake and distribution at the cellular level in the testes and bone marrow are shown in Figs. 3A and 3B, respectively. High concentrations of silver grains can be seen over and around the interstitial cells in the testes, but also over cells in the seminiferous tubule. Cells in the bone marrow are accumulating an extensive amount of indium (Fig. 3B), but in these cells the grains seem relatively uniformly distributed.

The electron microscope autoradiographs confirmed the suspicions that indium isotopes are internalized and retained in tissue cells. The results show that ^{114m}In accumulated in spermatogonia and in bone marrow cells as shown in Figs. 4A and 4B, respectively. In the spermatogonia, grains were found over the cell nucleus and in its immediate vicinity, as well as close to mitochondria.

DISCUSSION

The results in the present study represent situations in which the absorbed dose calculation based on conventional methods may underestimate or overestimate the absorbed dose to a fraction of cells in a specific organ. This may be particularly important if the cells to which the absorbed doses are underestimated are radiosensitive cells such as the hematopoietic stem cells in the red bone marrow or germ cells in the reproductive system. In light of the results in this paper, attention should be paid especially in situations where radionuclides emitting low-energy electrons are internalized by the cell.

Many physiologic and biochemical factors influence the *in vivo* localization and retention of a radiolabeled compound. In parallel studies we have found that the elimination of ^{111}In from tissues that have accumulated ^{111}In is slow (53,54). It has previously been established that ionic indium, like iron and gallium isotopes, binds to transferrin (Trf) in the plasma (66-68), and later is trans-chelated to this glycoprotein from different radiochelates and antibodies (69-71). It is likely that ^{111}In-transferrin identifies cells expressing

TABLE II
Percent Injected Activity in Rat Organs 5 Days Post-injection

Organ	^{111}In-Radiopharmaceutical				
	Chloride (n=7)	Oxine (n=3)	Tropolone (n=3)	CEA-F(ab')$_2$ (n=7)	
Testes	0.27±0.04	0.16±0.04	0.20±0.04	0.30±0.06	%/g
	(0.36±0.02)	(0.22±0.01)	(0.29±0.04)	(0.43±0.06)	%
Bone Marrow	1.00±0.05	0.91±0.04	0.85±0.04	0.93±0.095	%/g
	(7.38±0.35)	(6.78±0.29)	(5.89±0.71)	(7.42±0.74)	%
Spleen	1.18±0.04	4.76±0.04	1.68±0.04	1.62±0.06	%/g
	(1.00±0.04)	(2.24±0.10)	(1.02±0.10)	(1.05±0.10)	%
Liver	1.18±0.04	5.27±0.04	0.92±0.04	0.56±0.06	%/g
	(12.44±0.42)	(35.69±1.52)	(9.79±0.31)	(6.81±1.02)	%

transferrin receptors, TrfR, (72,73) and is taken up by receptor-mediated endocytosis (74-76). It is interesting to note that significant accumulation of indium takes place in tissues with cells expressing a large number of transferrin receptors, thus making them potential targets for ^{111}In-transferrin.

Notable tissues expressing transferrin receptors are the spleen and hematopoietic tissue, especially precursors to erythrocytes (77-79), basal epidermis, germ cells in the seminiferous tubules of the testis, Kupffer cells and hepatocytes. Macrophages in several tissues also appear to express receptors for transferrin (72). Presence of high affinity TrfRs on both murine and human macrophages has recently been confirmed, and it is assumed that TrfR expression may reflect macrophage immune activation (80). Monocyte-macrophages, together with other cells of the reticuloendothelial system, play a key role in the storage of iron, which is mostly derived from the breakdown of senescent red blood cells. This may explain the higher accumulation in the case of administered ^{111}In-oxine as described above. Transferrin receptors

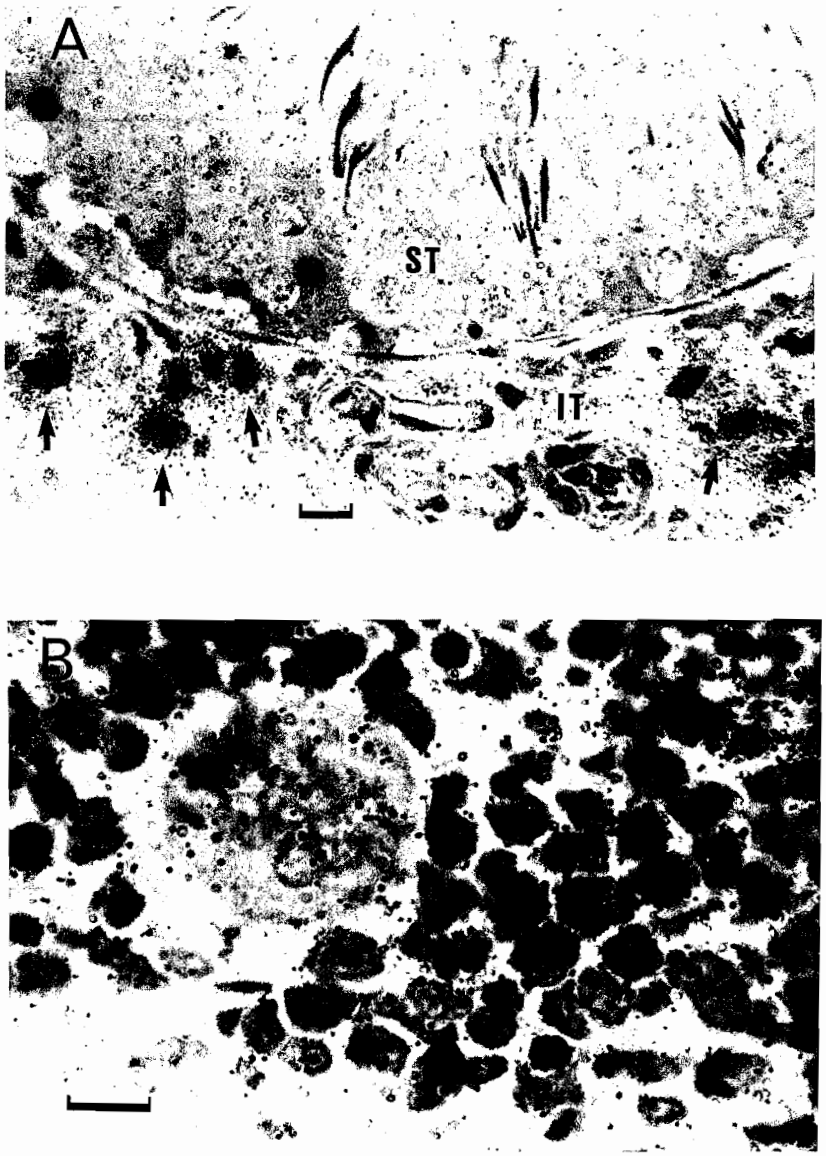

FIG. 3. Light-microscope autoradiographs illustrating the cellular localization of ^{114m}In in rat testes (A) and in a part of the red bone marrow (B). Several heavily labeled macrophages (arrows) are apparent in the interstitial tissue (IT) of the testes. Silver grains are also overlying cells in the seminiferous tubule (ST). The grains over the bone marrow cells seem to be relatively uniform, but some cells have a more intense accumulation. The large cell to the left is a megakaryocyte. Epon sections are stained with Richardson's azure II and methylene blue. Bars=10 μm.

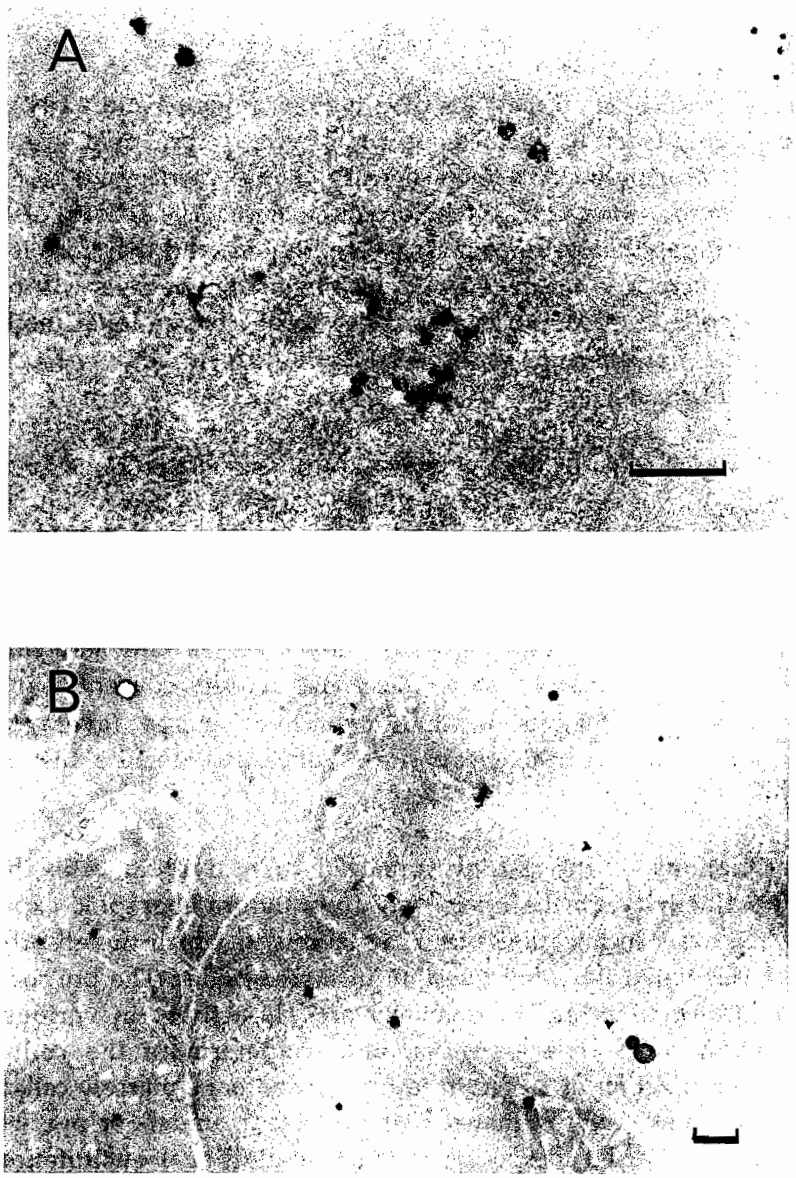

FIG. 4. Electron microscope autoradiographs showing uptake of ^{114m}In activity in a spermatogonial cell nucleus (A), and in bone marrow cells (B). In the spermatogonia silver grains were frequently found in the cell nucleus and its immediate vicinity. Bars=1 μm.

have also been identified in ovarian follicular cells (81). In the testes, Sertoli cells in the seminiferous tubules synthesize transferrin for delivery of iron to the developing germ cells (82), and may also be responsible for the transport of indium across the blood/testis barrier.

In our investigation the ^{111}In distribution in organs and parts of organs was measured in terms of the mean optical density. In principle, if the activity is uniformly distributed, the mean density should correspond to the mean absorbed dose to the organ or subregion of the organ. The activity distribution is, however, highly heterogeneous in several organs, and therefore it is likely that the absorbed dose to several cell clusters and single cells will be higher than the calculated average absorbed dose using conventional methods. At the same time, however, the absorbed dose to cells in "activity-free" regions will be overestimated.

It is possible to convert the measured optical density to cumulated activity (kBq-h) per unit area or, as in Fig. 5, per unit mass (65). Then the activity concentration for specific regions may be calculated and used as basic data for calculation of macroscopic absorbed doses to large cell clusters with an appropriate cell-to-cell calculation method (83-85). It is also possible to count grains in the micro-autoradiographs, however we did not make any estimation of the intracellular-to-extracellular activity concentration in this study because ^{114m}In emits β-radiation of high energy (average energy 777 keV) and therefore the decay site is uncertain despite the thin film emulsion.

Estimations of the energy imparted to individual cells that have accumulated activity can be made only from autoradiographic experiments showing the exact localization sites. The targets to which the absorbed dose should be calculated is a vital question in these studies. The purpose of this study was to examine the heterogeneity of ^{111}In-activity in various organs after injections of ^{111}In-substances, and to determine the cellular and subcellular localization of ^{114m}In in testes and red bone marrow cells. We did not, however, make any estimates of the degree of under- or over-estimates of the energy imparted to specific cells since additional quantitation of the cellular uptake should be done first with both microscopic autoradiography and subcellular fractionation before reliable and accurate calculations can be done.

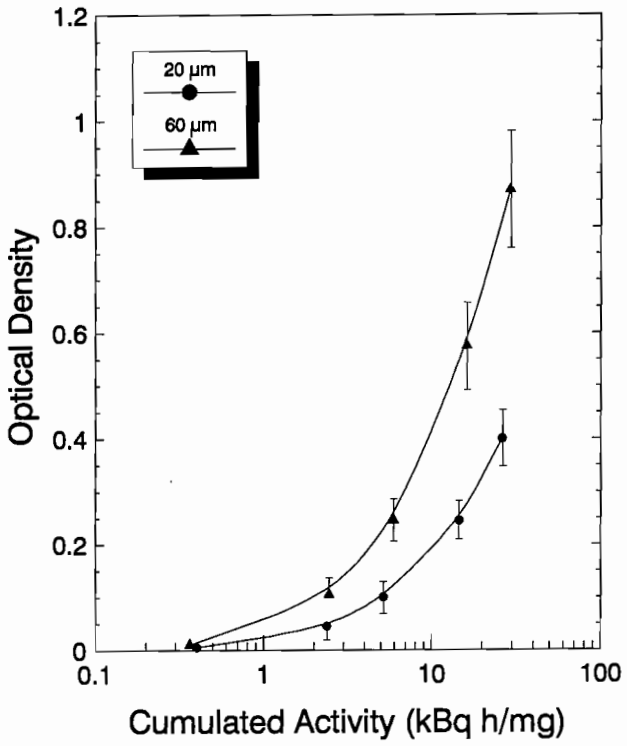

FIG. 5. Calibration curve for the autoradiographic film (Structurix D7) plotting optical density vs. cumulated ^{111}In-activity (*i.e.* exposure). Sectioned liver-homogenates with activities ranging from 3 to 300 Bq/mg, and of 20 µm and 60 µm were used for the calibration (65).

We found significant amounts of activity in interstitial cells, identified as macrophages. Very little is known about their differential radiosensitivity, although they are thought to be less radiosensitive than other hematopoietic cells (62). Spermatogonia are, however, known to be very radiosensitive, and it is interesting to note that besides activity in spermatogonia, the intense accumulation of indium in testicular interstitial cells may irradiate not only themselves, but also continuously expose stem cells and other cells in the spermatogenic cell lineage that are in the seminiferous tubule. Numerous cells in the bone marrow have been shown to accumulate large amounts of activity in both the cytoplasm and nucleus. In this study the cellular activity was not quantified, nor was the identity of the cells determined, but such investigations are presently under way.

CONCLUSIONS

In this new era of radiation protection (*i.e.* cell-level dosimetry) we must perform careful investigations of the cellular distribution of radioactivity and try to understand the biological behavior of different compounds at a microscopic level. In some cases it may be possible to use such data to introduce a dose-enhancement factor (5) specific for the radiopharmaceutical in question. In other cases, the high activity concentration in certain cells may need to be considered more harmful than we earlier thought it to be.

In conclusion, this study was the first attempt to examine the tissue distribution and cellular and subcellular localization after intravenously injected ^{111}In-radiopharmaceuticals. It was found that the activity was accumulated in a strikingly heterogeneous fashion in numerous organs and tissues. Thus, our experiments demonstrate that the distribution pattern may have a significant impact on calculation of the average absorbed dose to organs or individual cells, using conventional dosimetry. Finally, we suggest that autoradiographic techniques are excellent methods for acquiring localization data necessary for small scale dosimetry.

ACKNOWLEDGMENTS

The authors gratefully acknowledge the assistance of Mrs. Marianne Palmegren, at the Unit of Electron Microscopy, Department of Oncology, University of Lund. This work was in part supported by grants from the John and Augusta Persson Foundation for Medical Research, Lund, The Royal Physiographic Society, Lund, the Mrs. Berta Kamprad Foundation for Cancer Research, Lund, the Medical Faculty of Lund, and the Swedish Cancer Foundation, grant no. 2353-B91-05XAB and 3010-B91-01X.

REFERENCES

1. R. LOEVINGER and M. BERMAN, A revised schema for calculation of the absorbed dose from biologically distributed radionuclides. *MIRD Phamplet No. 1*, Revised. New York, Society of Nuclear Medicine, March 1976.

2. ICRU, *Methods of Assessment of Absorbed Dose in Clinical Use of Radionuclides*, Report 32, International Commission on Radiation Units and Measurements, Washington, D.C., 1979.
3. ICRP, *Radiation Dose to Patients from Radiopharmaceuticals*, Publication 53, The International Commission on Radiological protection Oxford, England: Pergamon Press, 1987.
4. ICRU, *Microdosimetry*, Report 36, International Commission on Radiation Units and Measurements Bethesda, MD, 1983.
5. D.V. RAO, G.F. GOVELITZ, and K.S.R. SASTRY, Radiotoxicity of thallium-201 in mouse testes: Inadequacy of conventional dosimetry. *J. Nucl. Med.* **24**, 145-153 (1983).
6. A.I. KASSIS, S.J. ADELSTEIN, C. HAYDOCK, and K.S.R. SASTRY, Thallium-201: an experimental and theoretical radiobiological approach to dosimetry. *J. Nucl. Med.* **24**, 1164-1175 (1983).
7. S.J. ADELSTEIN, A.I. KASSIS, and K.S.R. SASTRY, Cellular versus organ approaches to dose estimates. In *Proceedings of the Fourth Intenational Radiopharmaceutical Dosimetry Symposium* (A.T. Schlafke-Stelson and E.E. Watson, Eds.) Oak Ridge, TN, November 5-8, 1985; Oak Ridge: Oak Ridge Associated Universities, 1986:13-25. [CONF-851113-(DE86010102)].
8. G. MAKRIGIORGOS, S.J. ADELSTEIN, and A.I. KASSIS, Auger electron emitters: Insights gained from *in vitro* experiments. *Radiat. Environ. Biophys.* **29**, 75-91 (1990).
9. D.A. WEBER, K.F. ECKERMAN, L.T. DILLMAN, and J.C. RYMAN, *MIRD: Radionuclide data and decay schemes*. The Society of Nuclear Medicine, Inc. New York, 1989.
10. A. COLE, Absorption of 20-eV to 50,000-eV electron beams in air and plastic. *Radiat. Res.* **38**, 7-33 (1969).
11. M.J. BERGER, Distribution of absorbed dose around point sources and beta-particles in water and other media. *J. Nucl. Med.* (Suppl. No. 5), MIRD Pamphlet No. 7, 5-23 (1971).
12. W.W. HUNTER and X.J. RICCOBONO, Clinical evaluation of ^{111}In for localization of recognized neoplastic disease. *J. Nucl. Med.* **11**, 328 (1970).
13. D.A. GOODWIN, C.J. IMBORNE, and C.H. SONG, Comparative study of tumor and organ distribution of ^{111}In- and ^{67}Ga-labeled compounds in mice. *J. Nucl. Med.* **12**, 434 (1971).
14. D.A. GOODWIN, R. GOODE, L. BROWN, and C.J. IMBORNE, Indium-111-labeled transferrin for the detection of tumors. *Radiology*. **100**, 175-179 (1971).
15. P.A. FARRER, G.B. SAHA, and H.N. SHIBITA, Evaluation of ^{111}In-transferrin as a tumor scanning agent in humans. *J. Nucl. Med.* **13**, 429 (1972).
16. D.L. LILLIEN, H.G. BERGER, D.P. ANDERSON, and L.R. BENNETT, Indium-111-chloride: a new agent for bone marrow imaging. *J. Nucl. Med.* **14**, 184-186 (1973).
17. E.H. GILBERT, J.D. EARLE, M.L. GORIS, H.S. KAPLAN, and J.P. KRISS, The accuracy of ^{111}In-Cl3 as a bone marrow scanning agent. *Radiology*. **119**, 167-168 (1976).
18. M.L. THAKUR, J.P. LAVENDER, R.N. ARNOT, D.J. SILVESTER, and A.W. SEGAL, Indium-111-labeled autologous leukocytes in man. *J. Nucl. Med.* **18**, 1012-1019 (1977).
19 U. SCHEFFEL, P.A. MCINTYRE, B. EVATT, J.A. DVORNICKY, T.K. NATARAJAN, D.R. BOLLING, and E.A. MURPHY, Evaluation of Indium-111 as a new high photon

yield gamma-emitting "physiological" platelet label. *John Hopkins Med. J.* **140**, 285-293 (1977).

20. U. SCHEFFEL, M-F. TSAN, and PA. MCINTYRE, Labeling of human platelets with (111-In) 8-Hydroxyquinoline. *J. Nucl. Med.* **20**, 524-531 (1979).
21. M.K. DEWANJEE, S.A. RAO, and P. DISISHEIM, Indium-111 tropolone, a new high-affinity platelet label: Preparation and evaluation of labeling parameters. *J. Nucl. Med.* **22**, 981-987 (1981).
22. M.L. THAKUR, L. WALSH, H.L. MALECH, and A. GOTTSCHALK, Indium-111-labeled human platelets: improved method, efficacy and evaluation. *J. Nucl. Med.* **22**, 381-385 (1981).
23. J.E.T. BURKE, S. ROATH, D. ACKERY, and P. WYETH, The comparison of 8-hydroxyquinoline, tropolone, and acetylacetone as mediators in the labelling of polymorphonuclear leukocytes with Indium-111: A functional study. *Eur. J. Nucl. Med.* **7**, 73-76 (1982).
24. G.L. DETTMAN, B.L. VANDENBURG, R.D. JOHNSON, and G.W. MEYER, Indium-111-oxine labeled mouse spleen cells. *Int. J. Nucl. Med. Biol.* **8**, 137-144 (1981).
25. R.J.M. TENBERGE, A.T. NATARAJAN, S.L. YONG, M.R. HARDEMAN, E.A. VAN ROYEN, and P.Th.A. SCHELLEKENS, Labelling of human lymphocytes with 111-In-oxine. *Nuclear Geneeskundig Bullentin.* **4** (suppl), 18-20 (1982).
26. M.L. THAKUR, Radioisotopic labeling of platelets: A historical perspective. *Sem. Thromb. Hemost.* **9**, 79-85 (1983).
27. A.G. DESAI and M.L. THAKUR, Radiolabeled blood cells: Techniques and applications. *CRC Critical Reviews in Clinical Laboratory Sciences.* **24**, 95-122 (1986).
28. D.S. FAIRWEATHER, A.R. BRADWELL, P.W. DYKES, A.T. VAUGHAN, S.F. WATSON-JAMES, and S. CHANDLER, Improved tumour localization using indium-111 labeled antibodies. *Br. Med. J.* **287**, 167-170 (1983).
29. S.E. HALPERN, P.L. HAGAN, P.R. GARVER, J.A. KOZIOL, A.W.N. CHEN, J.M. FRINCKE, R.M. BARTHOLOMEW, G.S. DAVID, and T.H. ADAMS, Stability, characterization, and kinetics of 111-In-labeled monoclonal antitumor antibodies in normal animals and nude mouse-human tumor models. *Cancer Res.* **43**, 5347-5355 (1983).
30. S.E. HALPERN, The advantages and limits of Indium-111 labeling of antibodies Experimental studies and clinical applications. *Nucl. Med. Biol.* **13**, 195-201 (1986).
31. C.F. MEARES, Chelating agents for the binding of metal ions to antibodies. *Nucl. Med. Biol.* **13**, 311-318 (1986).
32. G.H. HINKLE, J.A. LOESCH, T.L. HILL, S.R. LEFEVRE and J.O. OLSEN, Indium-111-monoclonal antibodies in radioimmunoscintigraphy. *J. Nucl. Med. Tech.* **18**, 16-28 (1990).
33. D.J. HNATOWICH, Antibody radiolabeling, problems and promises. *Nucl. Med. Biol.* **17**, 49-55 (1990).
34. D.M. GOLDENBERG, In-vivo antibody imaging for detection of human tumors. In *Cancer Imaging with Radiolabeled Antibodies.* (D.M. Goldenberg, Eds.) pp. 293-312. Kluwer Academic Publishers, Norwell, MA, 1990.
35. Z.H. OSTER, S.C. SRIVASTAVA, P. SOM, G.E. MEINKEN, L.E. SCUDDER, K. YAMAMOTO, H.L. ATKINS, A.B. BRILL, and B.S. COLLER, Thrombus radioimmunoscintigraphy: An approach using monoclonal antiplatelet antibody. *Proc. Natl. Acad. Sci. USA.* **82**, 3465-3468 (1985).

36. A.M. PETERS, J.P. LAVENDER, S.G. NEEDHAM, I. LOUTFI, D. SNOOK, A.A. EPENETOS, P. LUMLEY, R.J. KEERY, and N. HOGG, Imaging thrombus with radiolabeled monoclonal antibody to platelets. *Br. Med. J.* **293**, 1525-1527 (1986).
37. M.L. THAKUR, P. THIAGARAJAN, F. WHITE III, C.H. PARK, and P.H. MAURER, Monoclonal antibodies for specific cell labeling: considerations, preparations and preliminary evaluation. *Nucl. Med. Biol.* **14**, 51-58 (1987).
38. M.L. THAKUR, M.D. RICHARD, and F.W. WHITE III, Monoclonal antibodies as agents for selective radiolabelling of human neutrophils. *J. Nucl. Med.* **29**, 1817-1825 (1988).
39. I. LOUTFI, J.R. BATCHELOR, J.P. LAVENDER, and A.A. EPENETOS, Lymphocyte targeting with 111-In-labeled monoclonal antiobodies. *Int. J. Cancer.* **2**, 45-49 (1988).
40. I. LOUTFI, P.M. CHISHOLM, D. BEVAN, and J.P. LAVENDER, *In vivo* imaging of rat lymphocytes with an indium 111-labeled anti-T cell monoclonal antibody: A comparison with indium 111-labeled lymphocytes. *Eur. J. Nucl. Med.* **16**, 69-76 (1990).
41. E. HINDIE, N. COLAS-LINHART, A. PETIET, and B. BOK, Microautoradiographic study of Technetium-99m colloid uptake by the rat liver. *J. Nucl. Med.* **29**, 1118-1121 (1988).
42. G.M. MAKRIGIORGOS, S. ITO, J. BARANOWSKA-KORTYLEWICZ, D.W. VINTER, A. IQBAL, A.D. VAN DEN ABBEELE, S.J. ADELSTEIN, and A.I. KASSIS, Inhomogeneous deposition of radiopharmaceuticals at the cellular level: Experimental evidence and dosimetric implications. *J. Nucl. Med.* **31**, 1358-1363 (1990).
43. B.A. JÖNSSON and S.E. STRAND, Biokinetics and tissue uptake of Indium-111 radiopharmaceuticals evaluated in the rat approaching radiation dosimetry at the cellular level [abstract]. *Eur. J. Nucl. Med. (suppl.)* **16**, S160, (1990).
44. A.W. SEGAL, P. DETEIX, R. GARCIA, P. TOOTH, G.D. ZANELLI, and A.C. ALLISON, Indium-111 labeling of leukocytes: a detrimental effect on neutrophil and lymphocyte function and an improved method of cell labeling. *J. Nucl. Med.* **19**, 1238-1244 (1978).
45. R.J.M. TENBERGE, A.T. NATARAJAN, M.R. HARDEMAN, E.A. VANROYEN, and P.TH.A. SCHELLEKENS, Labeling with Indium-111 has detrimental effects on human lymphocytes: concise communication. *J. Nucl. Med.* **24**, 615-620 (1983).
46. M. MEIGNAN and E. WIRQUIN, Lymphocyte radiolabeling: A challenge to their survival (letters to the editor). *J. Nucl. Med.* **28**, 1228-1229 (1987).
47. M.L. THAKUR, A.W. SEGAL, L. WELCH, M.J. LOUIS, J. HOPKINS, and T.J. PETERS, Indium-111-labeled cellular blood components: Mechanism of labeling and intracellular location in human neutrophils. *J. Nucl. Med.* **18**, 1020-1024 (1977).
48. D.V. RAO, K.S.R. SASTRY, H.E. GRIMMOND, R.W. HOWELL, G. GOVELITZ, V.K. LANKA, and V.B. MYLAVARAPU, Cytotoxicity of some indium radiopharmaceuticals in mouse testes. *J. Nucl. Med.* **29**, 375-384 (1988).
49. D.V. RAO, V.B. MYLAVARAPU, K.S.R. SASTRY. Internal Auger emitters: Effects on spermatogenesis and oogenesis in mice. In *DNA Damage by Auger Emitters* (K.F. Baverstock and D.E. Charlton, Eds), pp. 15-26. Taylor & Francis, London, 1988.
50. G. GRAFSTRÖM, A.M. EL HASSAN, B.A. JÖNSSON, S.E. STRAND, and J. TENNVALL, Rat testes as a radiobiological *in vivo* model for Auger electron emitting radionuclides. (Submitted).

51. G. GRAFSTRÖM, S.E. STRAND, J. TENNVALL, B.A. JÖNSSON, and H. LUNDGVIST, Radiobiological effects of ^{110}In versus ^{111}In in the rat testes. This volume.
52. D.V. RAO, V.R. NARRA, R.W. HOWELL, V.K. LANKA, and K.S.R. SASTRY. Induction of sperm head abnormalities by incorporated radionuclides: Dependence on subcellular distribution, type of radiation, dose rate, and presence of radioprotectors. *Radiat. Res.* **125**, 89-97 (1991).
53. B.A. JÖNSSON, S.E. STRAND, and L. ANDERSSON. Radiation dosimetry for ^{111}In-labeled F(ab')$_2$ fragments evaluated from tissue distribution in rats. *J. Nucl. Med.* (In press).
54. B.A. JÖNSSON and S.E. STRAND, Absorbed doses of ^{111}In and ^{114m}In after administration of ^{111}In-complexes with different biokinetics. J. Nucl. Med. (submitted).
55. H. JACKSON, N.C. JACKSON, I.D. MORRIS, and H.L. SHARMA. Intratesticular radionuclide and spermatogenic damage. *Br. Med. J.* **300** (1990).
56. L.C. JUNQUEIRA, J. CARNEIRO, and R.O. KELLEY, In *Basic Histology*, 6th ed. Appleton & Lange, Prentice-Hall International Inc., St. Mateo, CA, 1989.
57. M.L. MEISTRICH, N.R. HUNTER, N. SUZUKI, P.K. TROSTLE, and H.R. WITHERS, Gradual regeneration of mouse testicular stem cells after exposure to ionizing radiation. *Radiat. Res.* **74**, 349-362 (1978).
58. M. BIANCHI, Cytotoxic insult to germinal tissue. Part I. The Testes. In *Cytotoxic Insult to Tissue - Effects on Cell Lineages* (C.S. Potten and J.H. Hendry, Eds.) pp. 258-328, Churchill Livingstone, Edinburgh-London-Melbourne-New York, 1983.
59. ICRP, *Limits for Intakes of Radionuclides by Workers*, Report 30, Part 2, The International Commission on Radiological Protection, Oxford, England:Pergamon Press, 1980.
60. ICRP, *Radiation Dose to Patients from Radiopharmaceuticals*, Report 53, The International Commission on Radiological Protection. Oxford, England: Pergamon Press, 1987.
61. M. TAVASSOLI and J.M. YOFFEY, In *Bone Marrow: Structure and Function*, Alan R. Liss, Inc., New York, 1983.
62. J.H. HENDRY and B.I. LORD, The analysis of early and late response to cytotoxic insults in the haemopoietic cell hiearchy. In *Cytotoxic Insult to Tissue. Effects on cell lineages* (C.S. Potten and J.H. Hendry, Eds.), pp. 1-66, Churchill Livingstone, Edinburgh-London-Melbourne-New York, 1983.
63. S. ULLBERG, B. LARSSON, and H. TJÄVLE, Autoradiography. In *Biological Applications of Radiotracers* (H.J. Glenn and L.G. Colombetti, Eds.), part I, pp. 55-108. CRC Press Inc., Boca Raton, FL, 1982.
64. R. D'ARGY, G.O. SPERBER, B.S. LARSON, and S. ULLBERG. Computer-assisted quantification and image processing of whole body autoradiograms. *J. Pharmacol. Meth.* **24**, 165-181 (1990).
65. B.A. JÖNSSON, S.E. STRAND, and B.S. LARSSON. A quantitative autoradiographic study of the heterogeneous activity distribution of different Indium-111-labeled radiopharmaceuticals. *J. Nucl. Med.* (In press).
66. F. HOSAIN, P.A. McINTYRE, K. POULOSE, H.S. STERN, and H.N. WAGNER JR, Binding of trace amounts of ionic Indium-113m to plasma transferrin. *Clin. Chim. Acta*, **24**, 69-75 (1969).

67. R.D. WOCHNER, M. ADATEPE, A. VAN AMBERG, and E.J. POTCHEN, A new method for estimation of plasma volume with the use of the distribution space of indium-113m-transferrin. *J. Lab. Clin. Med.* **75**, 711-720 (1970).
68. R.W. EVANS and W. OGWANG, Interaction of indium with transferrin. *Biochem. Soc. Trans.* **16**, 833-823 (1988).
69. S.M. YEH, C.F. MEARES, and D.A. GOODWIN, Decomposition rates of radiopharmaceutical indium chelates in serum. *J. Radioanalyt. Chemistry.* **53**, 327-336 (1979).
70. W.C. COLE, S.J. DENARDO, C.F. MEARES, M.J. MCCALL, G.L. DENARDO, A.L. EPSTEIN, H.A. O'BRIEN, and M.K. MOI, Comparative serum stability of radiochelates for antibody radiopharmaceuticals. *J. Nucl. Med.* **28**, 83-90 (1987).
71. D.J. HNATOWICH, Biodistribution of 111-In-Labeled Monoclonal Antibodies - Letters to the Editor. *J. Nucl. Med.* **28**, 1924-1925 (1987).
72. K.C. GATTER, G. BROWN, I.S. TROWBRIDGE, R.E. WOOLSTON, and D.Y. MASON, Transferrin receptors in human tissues: their distribution and possible clinical relevance. *J Clin Pathol.* **36**, 539-545 (1983).
73. H.A. HUEBERS and C.A. FINCH, The physiology of transferrin and transferrin receptors. *Physiol Reviews.* **67**, 520-582 (1987).
74. S.M. LARSON, Z. GRUNBAUM, and J.S. RASEY, The role of transferrins in gallium uptake. *Int. J. Nucl. Med. Biol.* **8**, 257-266 (1981).
75. J.N. OCTAVE, Y.J. SCHNEIDER, A. TROUET, and R.R. CRICHTON, Iron uptake and utilization by mammalian cells. I: Cellular uptake of transferrin and iron. *Trend. Biochem. Sci. (TIBS).* **8**, 217-220 (1983).
76. R. WEINER, The role of transferrin and other receptors in the mechanism of Ga-67 localization. *Nucl. Med. Biol.* **17**, 141-149 (1990).
77. F.M. VAN BOCKXMEER and E.H. MORGAN, Identification of transferrin receptors in reticulocytes. *Biochim. Biophys. Acta.* **468**, 437-450 (1977).
78. S. DE ABREW, Assays for transferrin and transferrin receptors in tumour and other mouse tissues. *J. Nucl. Med. Biol.* **8**, 217-221 (1981).
79. J.N. OCTAVE, Y.J. SCHNEIDER, R.R. CRICHTON, and A. TROUET, Transferrin protein and iron uptake by isolated rat erythroblasts. *FEBS lett.* **137**, 119-123 (1982).
80. U. TESTA, M. PETRINI, M.T. QUARANTA, E. PELOSI-TESTA, G. MASTROBERARDINO, A. CAMAGNA, G. BOCCOLI, M. SARGIACOMO, G. ISACCHI, A. COZZI, P. AROSIO, and C. PESCHE, Iron up-modulates the expression of transferrin receptors during monocyte-macrophage maturation. *J. Biol. Chem.* **264**, 13181-13187 (1989).
81. S.L. ALESHIRE, K.G. OSTEEN, W.S. MAXSON, S.S. ENTMAN, C.A. BRADLEY, and F.F. PARL, Localization of transferrin and its receptor in ovarian follicular cells: morphologic studies in relation to follicular development. *Fertil. Steril.* **51**, 444-449 (1989).
82. C. MORALES, S.R. SYLVESTER, and M.D. GRISWOLD, Transport of iron and transferrin synthesis by seminiferous epithelium of the rat *in vivo*. *Biol. Reprod.* **37**, 995-1005 (1987).
83. K.S.R. SASTRY, C. HAYDOCK, A.M. BASHA, and D.V. RAO, Electron dosimetry for radioimmunotherapy: Optimal electron energy. *Radiat. Prot. Dosim.* **13**, 249-252 (1985).

84. M. MAKRIGIORGOS, S.J. ADELSTEIN, and A.I. KASSIS, Limitations of conventional internal dosimetry at the cellular level. *J. Nucl. Med.* 30, 1856-1864 (1989).

85. R.W. HOWELL, D.V. RAO, and K.S.R. SASTRY, Macroscopic dosimetry for radioimmunotherapy: Nonuniform activity distributions in solid tumors. *Med. Phys.* 16, 66-74 (1989).

DISCUSSION

Laster, B. H. Have you ever observed increased localization of the radiolabel in the adrenal gland? Your autoradiograph shows uptake in nasal epithelium and interstitium of testis which are associated with benzodiapapene receptors.

Strand, S. E. No, But perhaps we should.

Van den Abbeele, A. D. Which chelator did you use to label the monoclonal antibody? Did you see any nuclear localization of activity following injection of the antibody? Which of the ^{111}In labeled compounds showed intranuclear localization? In the case of DTPA, it has been reported that following metabolism in the liver, radiolabeled metabolites remain bound to cytoplasmic components.

Strand, S. E. We obtained our antibodies commercially (Scinhimum, Behringerwerhe, Marberg, Germany) with antibody conjugated with DTPA. So far in our experiments we believe that there is an intracellular and also a nuclear localization, although much smaller than compared to the other results due to the stronger bond between indium and antibody, and thus a much smaller transfer to transferrin.

Kassis, A. I. Being on the MIRD Committee, we have been aware of the possibility of dose nonuniformity for some radiopharmaceuticals. The problem is how to translate these expectations into humans undergoing diagnostic imaging. How will the nonuniform distribution you have seen in the animals be established in patients?

Strand, S. E. I think that we should, as much as possible, obtain tissue biopsies from patients (as we right now are doing for radiolabeled monoclonal antibodies) at the time of surgery. Detailed animal experimental studies must be done in order to extrapolate to the human situation with confirmation with biopsy data if possible.